

Predicting secondary organic aerosol formation from terpenoid ozonolysis with varying yields in indoor environments

Abstract The ozonolysis of terpenoids generates secondary organic aerosol (SOA) indoors. Models of varying complexity have been used to predict indoor SOA formation, and many models use the SOA yield, which is the ratio of the mass of produced SOA and the mass of consumed reactive organic gas. For indoor simulations, the SOA yield has been assumed as a constant, even though it depends on the concentration of organic particles in the air, including any formed SOA. We developed two indoor SOA formation models for single terpenoid ozonolysis, with yields that vary with the organic particle concentration. The models have their own strengths and were in agreement with published experiments for d-limonene ozonolysis. Monte Carlo analyses were performed, which simulated different residential and office environments to estimate ranges of SOA concentrations and yields for d-limonene and α -pinene ozonolysis occurring indoors. Results indicate that yields are highly variable indoors and are most influenced by background organic particles for steady-state formation and indoor ozone concentration for transient peak formation. Additionally, a review of ozonolysis yields for indoor-relevant terpenoids in the literature revealed much uncertainty in their values at low concentrations typical of indoors.

S. Youssefi, M. S. Waring

Department of Civil, Architectural and Environmental Engineering, Drexel University, Philadelphia, PA, USA

Key words: Fine and ultrafine particles; d-Limonene; α -Pinene; Oxidation; Modeling; Monte Carlo.

M. S. Waring
Department of Civil, Architectural and Environmental Engineering
Drexel University, 3141 Chestnut St.
Philadelphia, PA 19104
USA
Tel.: 011-215-895-1502
Fax: 011-215-895-1363
e-mail: msw59@drexel.edu

Received for review 20 December 2011. Accepted for publication 15 February 2012.

Practical Implications

The results in this study suggest important factors that govern indoor secondary organic aerosol (SOA) formation and yields, in typical residential and office spaces. This knowledge informs the development and comparison of control strategies to reduce indoor-generated SOA. The ranges of SOA concentrations predicted indoors allow the quantification of the effects of sorptive interactions of semi-volatile organic compounds or reactive oxygen species with SOA, filter loading owing to SOA formation, and impacts of SOA on health, if links are established.

Nomenclature

C_{Mb}	Indoor background organic particle mass concentration ($\mu\text{g}/\text{m}^3$)	E_{Mb}	Indoor mass emission rate of background organic particles ($\mu\text{g}/\text{h}$)
$C_{Mb,o}$	Outdoor background organic particle mass concentration ($\mu\text{g}/\text{m}^3$)	E_{O_3}	Indoor mass emission rate of ozone ($\mu\text{g}/\text{h}$)
C_{O_3}	Indoor ozone mole fraction (ppb)	E_{terp}	Indoor mass emission rate of terpenoids ($\mu\text{g}/\text{h}$)
$C_{O_3,o}$	Outdoor ozone mole fraction (ppb)	k	Reaction rate constant between ozone and terpenoid ($1/\text{ppb}\cdot\text{h}$)
C_{SOA}	Indoor secondary organic aerosol mass concentration ($\mu\text{g}/\text{m}^3$)	K_i	Gas-to-particle partitioning coefficient for terpenoid oxidation product i ($\text{m}^3/\mu\text{g}$)
C_{terp}	Indoor terpenoid mole fraction (ppb)	M_{org}	Organic aerosol mass concentration ($\mu\text{g}/\text{m}^3$)
$C_{\text{terp,o}}$	Outdoor terpenoid mole fraction (ppb)	p	Penetration factor of outdoor organic particles through the building envelope
C_V	Lumped indoor mass concentration of all volatile terpenoid oxidation products ($\mu\text{g}/\text{m}^3$)	ROG	Reactive organic gas concentration ($\mu\text{g}/\text{m}^3$)
$C_{\Delta\text{terp}}$	Lumped indoor mass concentration of all terpenoid oxidation products ($\mu\text{g}/\text{m}^3$)	t	Time (h)
$C_{\Delta\text{terp,ss}}$	Lumped indoor steady-state mass concentration of all terpenoid oxidation products ($\mu\text{g}/\text{m}^3$)	V	Volume of air (m^3)
		Y	SOA mass formation yield
		α_i	Mass stoichiometric coefficient for terpenoid oxidation product i
		β_{Mb}	Surface deposition rate of background organic particles ($1/\text{h}$)

β_{O_3}	Surface deposition rate of ozone (1/h)
β_{SOA}	Surface deposition rate of secondary organic aerosol (1/h)
Γ_{O_3}	Conversion factor to change between ppb and $\mu\text{g}/\text{m}^3$ for ozone
Γ_{terp}	Conversion factor to change between ppb and $\mu\text{g}/\text{m}^3$ for terpenoid
ΔM_{org}	Change in organic aerosol mass concentration because of terpenoid oxidation ($\mu\text{g}/\text{m}^3$)
ΔROG	Change in reactive organic gas concentration because of oxidation ($\mu\text{g}/\text{m}^3$)
Δt	Time step in numerical solution (h)
η_{Mb}	Filter removal efficiency of indoor background organic particles
$\eta_{\text{Mb,o}}$	Filter removal efficiency of outdoor background organic particles
η_{SOA}	Filter removal efficiency of indoor SOA
λ_i	Infiltration air exchange rate (1/h)
λ_n	Natural ventilation air exchange rate (1/h)
λ_r	Recirculation air exchange rate (1/h)
λ_v	Mechanical ventilation air exchange rate (1/h)

Introduction

Indoor airborne particles are transported from outdoors or are produced indoors by human activity or chemical reactions. One indoor source is secondary organic aerosol (SOA) formation, which results from ozonolysis of terpenoids (Chen and Hopke, 2009, 2010; Destailats et al., 2006; Fadeyi et al., 2009; Sarwar and Corsi, 2007; Sarwar et al., 2003; Wainman et al., 2000; Waring et al., 2008, 2011; Weschler and Shields, 1999; Zuraimi et al., 2007). Ozone/terpenoid reactions are important indoors (Weschler and Shields, 1996) and generate various products that form SOA by nucleation or partitioning mechanisms, increasing both particle number and mass. Ozone is transported indoors from outdoors (Weschler, 2000), or it may be emitted indoors by devices such as photocopiers, printers, and ion or ozone generators (Lee et al., 2001; Waring and Siegel, 2011; Waring et al., 2008). Terpenoids are unsaturated organics that are primarily emitted indoors by use of products such as cleaners and air fresheners (Nazaroff and Weschler, 2004).

There is no evidence linking indoor-formed SOA to health effects; however, outdoor-formed SOA is often a substantial portion of the urban particle mixture (Polidori et al., 2006) that has been correlated with health degradation (e.g., Pope and Dockery, 2006), so it is conceivable that indoor-formed SOA may influence health. Additionally, particles act as sorptive sinks for semi-volatile organic compounds (Weschler and Nazaroff, 2008) and/or reactive oxygen species (Chen et al., 2011). As SOA consists of ultrafine ($<0.1 \mu\text{m}$) and fine ($0.1\text{--}2.5 \mu\text{m}$) particles, it may increase exposure for either, because formed particles

of this size with sorbed species may penetrate deep in the lungs (Hinds, 1999). Finally, SOA contributes to in-duct filter loading, potentially altering filter reactivity with ozone over time. Accurately predicting SOA formation is thus an important aspect of understanding exposure to indoor pollution of various types.

Organic aerosol mass formation (ΔM_{org}) owing to reactive organic gas oxidation (ΔROG) may be parameterized with the fractional aerosol yield (Y), which Odum et al. (1996) expressed as the summed effects of gas-to-particle partitioning of individual products, i , of organic gas oxidation:

$$Y = \frac{\Delta M_{\text{org}}}{\Delta \text{ROG}} = M_{\text{org}} \sum_i \left(\frac{\alpha_i K_i}{1 + M_{\text{org}} K_i} \right). \quad (1)$$

Yield curves have mostly been fit to Equation 1 by assuming that formation is attributable to two hypothetical products (Griffin et al., 1999; Hoffmann et al., 1997; Odum et al., 1996) – one being the average of lower vapor pressure compounds and the other being the average of higher vapor pressure compounds. In this ‘two-product model’ fit, there are thus four fitting parameters: α_1 , K_1 , α_2 , and K_2 . Some researchers use ‘one-product model’ fits as well (e.g., Chen and Hopke, 2009, 2010). As shown in Equation 1, the yield is a function of and increases with any organic particle concentration (M_{org}), so the yield varies when the SOA concentration changes.

Indoor models often predict the rate of SOA formation as the product of the yield and the rate of terpenoid ozonolysis (e.g., Alshawa et al., 2007; Coleman et al., 2008; Fadeyi et al., 2009; Waring and Siegel, 2010). However, these models have limited accuracy because they assume a constant yield that is unaffected by the amount of organic particles in the air; incorporating varying yields into models such as these should increase their predictive power. In this article, after a brief review of yields in the literature for ozonolysis of common indoor terpenoids, we outlined two models that predict indoor SOA mass formation for single terpenoid ozonolysis with yields that vary as a function of the airborne organic particle concentration. We then validated those models with experimental data in the literature for d-limonene ozonolysis. We also used Monte Carlo analyses to estimate potential ranges of Y and C_{SOA} for scenarios typical of residential and office indoor environments.

Yields for ozonolysis of indoor terpenoids

Table 1 lists one- and two-product yield curve fits in the literature for ozonolysis of terpenoids relevant indoors. Photochemical reactions are generally unimportant indoors, and yields in Table 1 are for dark

Table 1 One- and two-product model yield curve fits for ozonolysis of terpenoids relevant indoors

Terpenoid	Fig. 1	α_1	K_1 ($\text{m}^3/\mu\text{g}$)	α_2	K_2 ($\text{m}^3/\mu\text{g}$)	Source
d-limonene	lim1	0.082	1	0.86	0.0055	1
d-limonene	lim2	0.969	0.0225	–	–	2
α -pinene		0.35	0.11	–	–	3
α -pinene		0.25	0.44	–	–	4
α -pinene		0.262	0.030	0.062	0.0028	5
α -pinene		0.125	0.088	0.102	0.0788	6
α -pinene	apin	0.14	0.26	0.14	0.036	7
β -pinene	pbin	0.026	0.195	0.485	0.003	8
Δ^3 -carene	d3car	0.128	0.337	0.068	0.0036	9
terpinolene	terpin	0.03	0.927	0.243	0.014	10

The label in the column “Fig. 1” describes the name of that terpenoid yield in Figure 1. Source: (1) Fit by authors using data from Leungsakul et al. (2005), Coleman et al. (2008), and Chen and Hopke (2010); (2) Chen and Hopke (2010); (3) Hoffmann et al. (1997); (4) Chen and Hopke (2009); (5) Yu et al. (1999); (6) Griffin et al. (1999); (7) Fit by authors using (3–6); (8, 9) Griffin et al. (1999); (10) Ng et al. (2006).

ozonolysis experiments. Two yield curve fits listed in Table 1 were determined for this article. For the first, a d-limonene yield curve (‘lim1’ in Table 1) was fit using the two-product model to yield data for d-limonene ozonolysis gathered from Leungsakul et al. (2005), Coleman et al. (2008), and Chen and Hopke (2010). For the second, the first four α -pinene fits on Table 1 were used to find an average α -pinene yield curve, to which a new two-product model was fit (‘apin’ in Table 1). Yield data comprising fits in Table 1 were collected over a large temperature range and with different particle detection methods. However, correcting the yields to the same reference condition is not feasible and was not attempted.

For the six terpenoids labeled in the column ‘Fig. 1’ in Table 1, their yield curves are plotted in Figure 1a as a function of the organic particle concentration (M_{org}). These yields will be known as Y_j in the text, where j is the terpenoid label. As shown, d-limonene has larger yields than other terpenoids, and Y_{lim1} and Y_{lim2} each reach as high as ~ 0.6 or 0.85 , respectively, as M_{org} increases. Y_{lim2} is larger than Y_{lim1} and is the yield from

the one-product model fit in Chen and Hopke (2010). Our α -pinene fit, Y_{apin} , behaves similarly to d-limonene yield curves when $M_{\text{org}} < \sim 25 \mu\text{g}/\text{m}^3$, but its upper limit of ~ 0.27 is lower. The final three terpenoid yields on Figure 1a are smallest in magnitude and are generally lower than ~ 0.2 for most of the shown ranges. Thus, the range of the yields depends markedly on which terpenoid is oxidized, and modeling SOA formation with a varying yield will mostly influence terpenoids with larger yield ranges.

To illustrate the contributions of each of the two products to the overall yield for Y_{lim1} , Figure 1b plots Y_{lim1} with the abscissa on a \log_{10} scale. The first product (α_1 and K_1) dominates when $M_{\text{org}} < \sim 20 \mu\text{g}/\text{m}^3$, and the second product (α_2 and K_2) governs when $M_{\text{org}} > \sim 20 \mu\text{g}/\text{m}^3$. Having well-quantified values for the first product of the two-product yield is therefore important as much indoor formation is likely to occur such that $M_{\text{org}} < \sim 20 \mu\text{g}/\text{m}^3$ (Nazaroff and Weschler, 2004). However, our value of $K_1 = 1 \text{ m}^3/\mu\text{g}$ was arbitrarily fit as there were no yield data for $M_{\text{org}} < 35 \mu\text{g}/\text{m}^3$ in results we used to fit Y_{lim1} . Hoffmann et al. (1997) remarked that the fit of the model line through the yield data was insensitive to the exact value of K_1 as long as $K_1 > \sim 0.1 \text{ m}^3/\mu\text{g}$. At higher values of M_{org} , this is true. However, this is not true at lower values of M_{org} . For instance, Figure 1c displays Y_{lim1} for three different values for K_1 (1, 5, and $20 \text{ m}^3/\mu\text{g}$), but with the abscissa plotted on a \log_{10} scale to $10 \mu\text{g}/\text{m}^3$. The different values of K_1 influence the resulting yield curves at these low M_{org} , and the lack of yield data for conditions when $M_{\text{org}} < 35 \mu\text{g}/\text{m}^3$ is a gap in the literature. Additionally, we showed Y_{lim2} to illustrate that this one-product model results in low yields when M_{org} is low, even though it has high yields at higher M_{org} .

Modeling methodology

We developed two SOA formation models, SOA-M1 and SOA-M2, which account for the ozonolysis of a

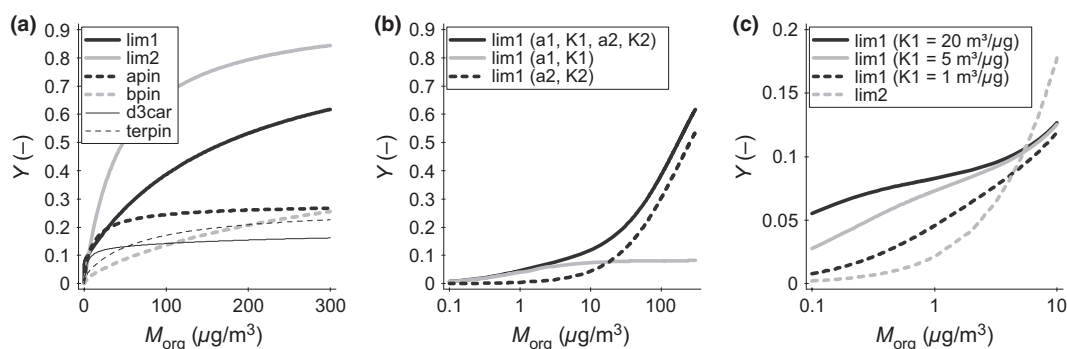


Fig. 1 Secondary organic aerosol (SOA) yields, Y , as a function of total organic particle concentration, M_{org} ($\mu\text{g}/\text{m}^3$), for the ozonolysis of indoor-occurring terpenoids. Yield curves are one- or two-product model fits in Table 1, which also lists our terpenoid naming convention. Individual plots show (a) yields of six terpenoids vs. M_{org} with the abscissa on a linear scale; (b) Y_{lim1} , as well as the individual products in the two-product model for Y_{lim1} , vs. M_{org} with the abscissa on a \log_{10} scale; and (c) Y_{lim1} , Y_{lim2} , as well as Y_{lim1} for two different values of K_1 (5 and 20 instead of $1 \text{ m}^3/\mu\text{g}$), vs. M_{org} with the abscissa on a \log_{10} scale

single terpenoid. First, elements common to both models are introduced, and then elements unique to each model are developed. Finally, our Monte Carlo approach is discussed.

Assumptions and equations common to both SOA formation models

The indoor air is assumed at constant temperature and density and as well mixed. Gas-phase compound sorption to building surfaces was neglected. Volume-normalized mass balances were written for ozone, terpenoid, and background organic particles, in either mole fractions or mass concentration form, and are Equations 2–4, respectively:

$$\frac{dC_{O_3}}{dt} = (\lambda_i + \lambda_n + \lambda_v)C_{O_3,o} + \frac{E_{O_3}}{V} \frac{1}{\Gamma_{O_3}} - (\lambda_i + \lambda_n + \lambda_v + kC_{terp} + \beta_{O_3})C_{O_3} \quad (2)$$

$$\frac{dC_{terp}}{dt} = (\lambda_i + \lambda_n + \lambda_v)C_{terp,o} + \frac{E_{terp}}{V} \frac{1}{\Gamma_{terp}} - (\lambda_i + \lambda_n + \lambda_v + kC_{O_3})C_{terp} \quad (3)$$

$$\frac{dC_{Mb}}{dt} = (p\lambda_i + \lambda_n + (1 - \eta_{Mb,o})\lambda_v)C_{Mb,o} + \frac{E_{Mb}}{V} - (\lambda_i + \lambda_n + \lambda_v + \eta_{Mb}\lambda_r + \beta_{Mb})C_{Mb}. \quad (4)$$

In Equations 2–4, the terms on the left-side are the rate of changes in C_{O_3} , C_{terp} , and C_{Mb} . On the right side, the positive terms are sources and negative terms are losses. All species may have sources owing to outdoor-to-indoor transport with infiltration, natural and mechanical ventilation air, or owing to direct indoor emission. Losses of C_{O_3} include all air exchange terms, reaction with C_{terp} , and reaction with indoor surfaces. Ozone attenuation as air passes through the envelope with infiltration air or through the HVAC system with mechanical ventilation air was neglected because of uncertainty in their magnitudes, but can easily be incorporated if desired. Losses of C_{terp} are similar except it does not react on surfaces. Losses of C_{Mb} include air exchange, as well as removal to the recirculation air filter and to indoor surfaces. In Equations 2 and 3, concentrations are in mole fractions but their emissions are in units of mass per time, so conversion factors, Γ_{O_3} and Γ_{terp} , are used when necessary.

Modeling SOA formation with SOA-M1

The first SOA formation model is similar in form to that which is commonly employed in constant yield models. In this approach, we begin with a volume-normalized mass balance for C_{SOA} , which is Equation 5:

$$\frac{dC_{SOA}}{dt} = YkC_{O_3}C_{terp}\Gamma_{terp} - (\lambda_i + \lambda_n + \lambda_v + \eta_{SOA}\lambda_r + \beta_{SOA})C_{SOA} \quad (5)$$

In Equation 5, the source of C_{SOA} is attributable to the ozone/terpenoid reactions occurring indoors. Losses in Equation 5 include those that are attributable to air exchange, removal to an HVAC filter in the recirculation air stream, and surface deposition. Although SOA is present in outdoor air in urban areas (Polidori et al., 2006), our focus is indoor formation. If desired, outdoor SOA can be included in SOA-M1 or SOA-M2 as part of the outdoor concentration of background organic particles in Equation 4. For the yield, we use the two-product form:

$$Y = \frac{\Delta C_{SOA}}{\Delta C_{terp}} = (C_{SOA} + C_{Mb}) \left(\frac{\alpha_1 K_1}{1 + (C_{SOA} + C_{Mb})K_1} + \frac{\alpha_2 K_2}{1 + (C_{SOA} + C_{Mb})K_2} \right). \quad (6)$$

The rightmost side of Equation 6 represents the two-product form of the incremental increase in the SOA mass concentration for a corresponding incremental decrease in the terpenoid mass concentration. For SOA-M1, it is substituted for Y into Equation 5 and then Equations 2–5 are solved simultaneously to find C_{SOA} , using the Runge–Kutta order 4 (RK4) numerical method.

Modeling SOA formation with SOA-M2

Kroll and Seinfeld (2005) expressed SOA formation as a function of the ΔROG reacted for outdoor chemistry. We have modified their approach for indoor environments. Rather than tracking C_{SOA} with time, SOA-M2 tracks the change with time in the concentration of products owing to terpenoid ozonolysis indoors. We begin with the concept that ozone and terpenoids react to form a single, hypothetical product, $C_{\Delta terp}$ ($\mu g/m^3$), which is a lumped concentration of all products of the oxidized terpenoid that remains indoors at a particular instant in time, assuming that this product has the same molecular weight as the parent terpenoid. In outdoor air or batch reactor systems with negligible losses owing to air exchange and deposition, $C_{\Delta terp} = \Delta ROG$. There are losses indoors because of air exchange, deposition, and filtration, so $C_{\Delta terp} < \Delta ROG$. Some of $C_{\Delta terp}$ will exist in the particle-phase as C_{SOA} , and some of it will exist in the gas-phase as volatile products, C_v , at fractions that depend on the amount of $C_{\Delta terp}$ indoors. Partitioning was derived as an equilibrium process. So, as $C_{\Delta terp}$ changes in the indoor air, the relative fractions

of C_{SOA} and C_V adjust to the current condition. For particles of the size of SOA ($< 1 \mu\text{m}$), the timescale for a sorption process to adjust to equilibrium is $< 1 \text{ min}$ (Weschler and Nazaroff, 2008), which is much less than the residence time of air indoors (Murray and Burmaster, 1995; Persily et al., 2006), so we assume instantaneous adjustment.

To determine C_{SOA} as a function of $C_{\Delta\text{terp}}$, we recognize that Equation 6 holds not only for incremental changes in products and reactants but also for instantaneous equilibrium partitioning of products (Hoffmann et al., 1997; Kroll and Seinfeld, 2005), as in Equation 7:

$$\frac{C_{\text{SOA}}}{C_{\Delta\text{terp}}} = (C_{\text{SOA}} + C_{\text{Mb}}) \left(\frac{\alpha_1 K_1}{1 + (C_{\text{SOA}} + C_{\text{Mb}}) K_1} + \frac{\alpha_2 K_2}{1 + (C_{\text{SOA}} + C_{\text{Mb}}) K_2} \right). \quad (7)$$

For a similar expression (Equation 4 in their work), Kroll and Seinfeld (2005) solved for C_{SOA} considering one- and two-product yield models, both without and with organic matter present besides the SOA, yielding four algebraic expressions. For instance, with no other organic particles, the solution to Equation 7 is quadratic (Kroll and Seinfeld, 2005) and is:

$$C_{\text{SOA}} = \frac{1}{2} \left(C_{\Delta\text{terp}} (\alpha_1 + \alpha_2) - \frac{1}{K_1} - \frac{1}{K_2} \right) + \frac{\left[4K_1 K_2 (K_1 \alpha_1 C_{\Delta\text{terp}} + K_2 \alpha_2 C_{\Delta\text{terp}} - 1) + (K_1 + K_2 - K_1 K_2 C_{\Delta\text{terp}} (\alpha_1 + \alpha_2))^2 \right]^{\frac{1}{2}}}{2K_1 K_2} \quad (8)$$

We do not reproduce their other solutions, but in other situations, SOA-M2 could use the Kroll and Seinfeld (2005) one-product yield solutions for C_{SOA} when $C_{\text{Mb}} \approx 0$ or $C_{\text{Mb}} > 0 \mu\text{g}/\text{m}^3$, or their two-product solution to Equation 7 when $C_{\text{Mb}} > 0 \mu\text{g}/\text{m}^3$ (which is cubic with many terms). As at any point in time, $C_{\text{SOA}} = Y C_{\Delta\text{terp}}$ and $C_V = (1 - Y) C_{\Delta\text{terp}}$, we derived a differential equation for $C_{\Delta\text{terp}}$ by substituting $Y C_{\Delta\text{terp}}$ for C_{SOA} into Equation 5 and computing the derivative of $d(Y C_{\Delta\text{terp}})/dt$, which when rearranged results in Equation 9:

$$\frac{dC_{\Delta\text{terp}}}{dt} = k C_{\text{O}_3} C_{\text{terp}} \Gamma_{\text{terp}} - \left(\lambda_i + \lambda_n + \lambda_v + \eta_{\text{SOA}} \lambda_r + \beta_{\text{SOA}} + \frac{1}{Y} \frac{dY}{dt} \right) C_{\Delta\text{terp}}. \quad (9)$$

The source of $C_{\Delta\text{terp}}$ is from the ozone/terpenoid reactions and losses are attributable to air exchange, as well as filtration and deposition mechanisms and the

term $(1/Y) (dY/dt)$. Equation 9 therefore implies that all products of terpenoid oxidation, not just the SOA-phase products, are subject to particle loss mechanisms. To understand this point more, we derived a similar expression for C_V , using the fact that $dC_{\Delta\text{terp}}/dt = (dC_{\text{SOA}}/dt + dC_V/dt)$:

$$\frac{dC_V}{dt} = (1 - Y) k C_{\text{O}_3} C_{\text{terp}} \Gamma_{\text{terp}} - \left(\lambda_i + \lambda_n + \lambda_v + \eta_{\text{SOA}} \lambda_r + \beta_{\text{SOA}} + \frac{1}{Y(1 - Y)} \frac{dY}{dt} \right) C_V. \quad (10)$$

Therefore, beyond air exchange effects, the volatile products, C_V , are affected by the loss terms: $\{\eta_{\text{SOA}} \lambda_r + \beta_{\text{SOA}} + 1/[Y(1 - Y)] [dY/dt]\}$. Particle losses applying to volatile products may seem counterintuitive; however, C_V is affected by particle-specific loss mechanisms because partitioning is an equilibrium process. As C_{SOA} is lost to filters or surfaces, there is a driving force for some of the C_V to further partition to the SOA phase, at a fraction dependent on the total amount of $C_{\Delta\text{terp}}$ currently indoors. At steady state when $dY/dt = 0$, the amount of C_V that further partitions to the SOA phase is equivalent to the loss term $(\eta_{\text{SOA}} \lambda_r + \beta_{\text{SOA}})$. When not at steady state, the loss of C_V owing to this further partitioning is increased if $dY/dt > 0$ (when $C_{\Delta\text{terp}}$ is increasing)

and decreased if $dY/dt < 0$ (when $C_{\Delta\text{terp}}$ is decreasing) by the term $(1/(Y(1 - Y))) (dY/dt)$.

Solving Equations 2–4 and 9 simultaneously with the RK4 numerical method gives us C_{O_3} , C_{terp} , C_{Mb} , and $C_{\Delta\text{terp}}$ during the modeled time. Then, once $C_{\Delta\text{terp}}$ and C_{Mb} are known at each time step, one of the algebraic solutions to Equation 7 from Kroll and Seinfeld (2005) (e.g., Equation 8) can be used to solve for C_{SOA} at any time. One important point is that the RK4 transient solution for $C_{\Delta\text{terp}}$ with Equation 9 uses values for Y and dY/dt that were determined from the transient yields of the solution from SOA-M1. Because using SOA-M2 requires prior knowledge of the time-resolved yields in some way, one might wonder at its utility. However, the strength of SOA-M2 is that it can easily be used to solve for C_{SOA} at steady state with an algebraic solution, which cannot be performed with SOA-M1 because of the interdependence of Y and C_{SOA} in Equations 5 and 6. To do so, Equation 9 is solved to obtain $C_{\Delta\text{terp}}$ at steady state, which is Equation 11:

$$C_{\Delta\text{terp,ss}} = \frac{kC_{\text{O}_3}C_{\text{terp}}\Gamma_{\text{terp}}}{\lambda_i + \lambda_n + \lambda_v + \eta_{\text{SOA}}\lambda_r + \beta_{\text{SOA}}} \quad (11)$$

Then, one may solve for C_{SOA} with an algebraic or iterative solution to Equation 7.

Monte Carlo analyses

Considering ozonolysis of d-limonene and α -pinene separately, we conducted Monte Carlo analyses with probability distributions as inputs to find typical ranges of yields and C_{SOA} . Three residences and one office were simulated, which were differentiated by their air exchange rates and sources of organic particles besides SOA and are as follows:

- R1: Residence; natural ventilation air exchange; and source of organic particles from air exchange with outdoor air.
- R2: Residence; infiltration and recirculation air exchange; and source of organic particles from air exchange with outdoor air.
- R3: Residence; infiltration and recirculation air exchange; and source of organic particles from air exchange with outdoor air and indoor smoking.
- O1: Office; infiltration, mechanical ventilation, and recirculation air exchange; and source of organic particles from air exchange with outdoor air.

For each of these, steady-state formation because of air freshener use and transient formation because of use of a general purpose cleaner were modeled. The input distributions used in the Monte Carlo analyses that varied by scenario are listed in Table 2, and constant distributions and parameters are listed in the table notes. Details on derivations of all parameters are provided in Data S1.

Results and discussion

Validation of SOA formation models

To explore the validity of SOA-M1 and SOA-M2, we simulated transient and steady-state experiments in the literature for d-limonene ozonolysis, using a yield of Y_{lim1} and $k = 0.0183/\text{ppb/h}$ at 25°C (Atkinson et al., 1990). Transient results were evaluated by modeling a case from Singer et al. (2006a) who measured transient formation owing to ozonolysis of an orange-oil degreaser (OOD), which contained d-limonene as the only reactive gas, in a 50-m^3 mock room. Model inputs were $\lambda_v = 1/\text{h}$, $\beta_{\text{O}_3} = 1/\text{h}$, $C_{\text{O}_3,\text{o}} = 130$ ppb, an initial $C_{\text{O}_3} = 65$ ppb at $t = 0$ h, and $C_{\text{terp}} = 1100$ ppb until $t = 0.67$ h (from their Figure 1). Formation was modeled using different time steps (Δt) with the RK4 numerical solution to test for convergence, and select results with different Δt are shown along with measured

Table 2 Scenario-specific input parameters for Monte Carlo analyses exploring SOA formation owing to steady and transient ozonolysis of d-limonene and α -pinene, including geometric means (and geometric standard deviations) of lognormal input distributions

Parameter ^a	HVAC operation and indoor organic particle emission			
	Scenario ^b R1	Scenario R2	Scenario R3	Scenario O1
λ_i (1/h)	0	0.53 (2.27) ^c	0.53 (2.27) ^c	0.25 (1.5) ^e
λ_n (1/h)	2.2 (1.5) ^f	0	0	0
λ_v (1/h)	0	0	0	0.73 (1.8) ^e
λ_r (1/h)	0	1.5 (1.9) ^d	1.5 (1.9) ^d	3.0 (1.5) ^e
η_{SOA}	0	0.10 (3.55) ^e	0.10 (3.55) ^e	0.10 (3.55) ^e
η_{Mb}	0	1.55 $\cdot\eta_{\text{SOA}}$ ^e	1.55 $\cdot\eta_{\text{SOA}}$ ^e	1.15 $\cdot\eta_{\text{SOA}}$ ^e
$\eta_{\text{Mb,o}}$	0	0	0	1.13 $\cdot\eta_{\text{SOA}}$ ^e
E_{Mb}/V ($\mu\text{g}/\text{m}^3\cdot\text{h}$)	0	0	18.5 (1.96) ^f	0
Terpenoid emission ^g				
	Steady	Transient		
E_{terp}/V ($\mu\text{g}/\text{m}^3\cdot\text{h}$)	36.8 (2.29) ^h			
Mass emitted (mg)		168 (1.58) ^h		
Time emitted (min)		4.33 (1.32) ^h		

Input parameters that do not vary by scenario are in table notes, and symbols are defined in Nomenclature section.

SOA, secondary organic aerosol.

^aConstant input distributions and parameters are $C_{\text{O}_3,\text{o}} = 25.5$ ppb (2.04) with max of 130 ppb; $C_{\text{Mb,o}} = 3.15$ $\mu\text{g}/\text{m}^3$ (1.9) (EPA monitoring sites); $\beta_{\text{O}_3} = 2.5/\text{h}$ (1.5) with range of 0.95–8.05/h (Lee et al., 1999; Morrison et al., 2011); $p = 0.72$, $\beta_{\text{SOA}} = 0.060/\text{h}$ (1.5), $\beta_{\text{Mb}} = 0.14/\text{h}$ (1.5) (Coleman et al., 2008; Lai and Nazaroff, 2000; Liu and Nazaroff, 2001; Riley et al., 2002; Waring and Siegel, 2008, 2010). Terpenoid reaction rate constants (k) were 0.0183/ppb/h for d-limonene and 0.0076/ppb/h for α -pinene (Atkinson et al., 1990), and yields were Y_{lim1} and Y_{apin} (from Table 1).

^bScenario R1: residence with natural ventilation air exchange, and organic particles from outdoors; R2: residence with infiltration and recirculation air exchange, and organic particles from outdoors; R3: same as R2 but with organic particles also from indoor smoking; and O1: office with infiltration, mechanical ventilation, and recirculation air exchange, and organic particles from outdoors.

^cRiley et al. (2002) and Murray and Burmaster (1995).

^dStephens et al. (2011).

^eWaring and Siegel (2008, 2010).

^fHolcomb (1993).

^gValues are for d-limonene emissions; identical values were used for α -pinene emissions for direct comparison.

^hSinger et al. (2006b); for transient emissions, results from these two distributions, along with the volume of 50 m^3 from Singer et al. (2006b) were used to calculate the E_{terp}/V , which was operational for its particular time of emission and then set to zero.

results in Figure 2. Convergence essentially occurs when $\Delta t \geq 10^{-3}$ h; peak formation for $\Delta t = 10^{-3}$ h is within 98% of that for $\Delta t = 10^{-4}$ h, which was 99.9% of the result for $\Delta t = 5 \times 10^{-5}$ h (not shown). The predicted and measured C_{SOA} peaks are 253 and 270 $\mu\text{g}/\text{m}^3$, respectively, with a 6.3% difference.

We also simulated the Singer et al. (2006a) case to confirm that SOA-M1 and SOA-M2 produced identical results for C_{SOA} , as well as $C_{\Delta\text{terp}}$ and C_V . For SOA-M1, C_{SOA} and Y were determined with Equations 5 and 6, respectively, and then $C_{\Delta\text{terp}} = C_{\text{SOA}}/Y$ and $C_V = C_{\text{SOA}}/Y - C_{\text{SOA}}$. For SOA-M2, time-resolved values of Y from SOA-M1 were used in the calculations of $C_{\Delta\text{terp}}$ and C_V with Equations 9 and 10. Then, Equation 8 was used to find C_{SOA} . We chose to compare the results of the two models for a condition without background organic particles as the

two-product solution of Equation 7 when $C_{Mb} > 0 \mu\text{g}/\text{m}^3$ is cubic and difficult to work with practically. Results for C_{SOA} , $C_{\Delta\text{terp}}$, and C_V using SOA-M1 and

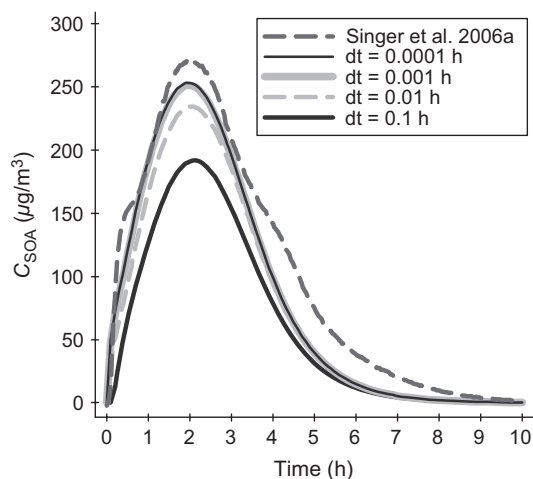


Fig. 2 Modeled and measured results of transient secondary organic aerosol (SOA) concentrations, C_{SOA} ($\mu\text{g}/\text{m}^3$), vs. time (h) for the orange-oil degreaser case from Singer et al. (2006a). SOA formation was predicted with SOA-M1, with model details and inputs described in the text. The four lines labeled as different values of ‘dt’ in the legend display predicted outcomes using different time steps (Δt) with the Runge–Kutta order 4 numerical solution. The line labeled ‘Singer et al., 2006a’ represents the measured data supplied by the authors

SOA-M2 were identical, and C_{SOA} was similar to converged solutions displayed in Figure 2.

Experiments with d-limonene ozonolysis from Fadeyi et al. (2009), Coleman et al. (2008), and Li et al. (2002) were used to validate steady-state solutions of SOA-M1 and SOA-M2. Fadeyi et al. (2009) measured formation in a 266-m^3 simulated office while varying ventilation, recirculation, and filtration parameters. Coleman et al. (2008) determined formation in a 198-l chamber from ozonolysis of the OOD used in Singer et al. (2006a). Li et al. (2002) assessed formation at low and high air exchange rates in a 29-m^3 office. For these 24 experiments, the experimental ID (from original article), model inputs, reported C_{SOA} , and predicted C_{SOA} and Y are listed in Table 3. Background particles were neglected owing to uncertainty in values. Steady-state C_{SOA} were found with SOA-M1 by running the RK4 solution until steady conditions were reached ($\Delta t = 0.1$ h, which converged). Finding steady solutions with SOA-M2 was algebraic. Equation 11 was used to find $C_{\Delta\text{terp,ss}}$, and then C_{SOA} was determined with Equation 8. Both models predicted identical values, with the exception of the italicized entries in Table 3, which are from SOA-M1. SOA-M2 actually predicts $C_{SOA} < 0 \mu\text{g}/\text{m}^3$ with Equation 8 when $C_{\Delta\text{terp}}$ is low. This non-physical result is indicative of the unsuitability of our (arbitrary) K_1 value, because of the

Table 3 Experimental conditions and measured SOA formation from studies in the literature used evaluate predicted SOA concentrations and yields from SOA-M1 and SOA-M2

Exp. no ^a	Exp. ID ^b	Reported values from literature studies							Predicted values ^c	
		C_{O_3} (ppb)	C_{terp} (ppb)	λ_v^d (/h)	λ_r (/h)	η_{SOA}	β_{SOA} (/h)	C_{SOA} ($\mu\text{g}/\text{m}^3$)	C_{SOA} ($\mu\text{g}/\text{m}^3$)	Y
1	LVLR/None	290	16	2.6	7	0	0.5	34	32	0.21
2	LVLR/New	165	22	2.6	7	0.37	0.5	6	6.6	0.10
3	LVLR/Used	175	21	2.6	7	0.34	0.5	5	7.2	0.10
4	LVHR/None	110	19	4.4	14	0	1	6	3.0	0.075
5	LVHR/New	100	20	4.4	14	0.4	1	2	0.7	0.036
6	LVHR/Used	98	20	4.4	14	0.39	1	3	0.7	0.036
7	HVLR/None	78	29	3.6	7	0	0.5	13	5.2	0.093
8	HVLR/New	70	30	3.6	7	0.37	0.5	1	2.1	0.065
9	HVLR/Used	70	30	3.6	7	0.34	0.5	1	2.2	0.067
10	HVHR/None	37	28	5.4	14	0	1	4	0.5	0.029
11	HVHR/New	40	27	5.4	14	0.4	1	1	<0.001	<0.001
12	HVHR/Used	36	28	5.4	14	0.39	1	1	<0.001	<0.001
13	OOD-HH	21	518	3	0	0	0	259	195	0.53
14	OOD-HL	7	588	1	0	0	0	203	239	0.57
15	OOD-MH	11	528	3.1	0	0	0	92	52	0.27
16	12/16/1999	125	160	15	0	0	0.43	17	23	0.18
17	12/29/1999	100	1	15	0	0	0.43	0.2	<0.001	<0.001
18	1/13/2000	100	240	15	0	0	0.43	45	34	0.22
19	1/19/2000	100	210	15	0	0	0.43	12	26	0.19
20	1/27/2000	80	205	2	0	0	0.43	>350	489	0.71
21	2/4/2000	80	360	2	0	0	0.43	>350	978	0.81
22	2/11/2000	2	270	2	0	0	0.43	4	1.1	0.05
23	2/15/2000	175	125	2	0	0	0.43	>350	704	0.77
24	2/16/2000	125	175	2	0	0	0.43	>350	704	0.77

OOD, orange-oil degreaser; SOA, secondary organic aerosol.

^aExperiments 1–12 are from Fadeyi et al. (2009); Experiments 13–15 are from Coleman et al. (2008); Experiments 16–24 are from Li et al. (2002).

^bExperiment ID is the same as that in the original paper.

^cSOA-M1 and SOA-M2 predict identical results and are only listed once except for italicized values, which are results from SOA-M1. See text for more details.

^dFor Fadeyi et al. (2009), λ_v equals the sum of ventilation and duct leakage rates.

lack of low M_{org} data. As K_1 increases, this $C_{\Delta\text{terp}}$ threshold to achieve meaningful results decreases.

To assess the model performance, we used the ASTM method D5157-91 (ASTM 1991), which compares measured and predicted values, recommending there is a (i) slope of 0.75–1.25 and intercept within 25% of average value; (ii) correlation coefficient (r) ≥ 0.9 ; (iii) normalized mean square error (NMSE) ≤ 0.25 ; and (iv) fractional bias (FB) ≤ 0.25 . For the predicted values of Singer et al. (2006a), results were slope = 0.96, intercept % = 17%, $r = 0.99$, NMSE = 0.064, and FB = -0.20. For the 20 steady-state cases, excluding four from Li et al. (2002) over the detection limit, the results were slope = 0.89, intercept % = 0.006%, $r = 0.96$, NMSE = 0.33, and FB = -0.12. This analysis implies there is a slight bias to under-predict values, but the predicted results are generally in good agreement with the measured ones, especially given the uncertainty in some inputs and reported values. For instance, in Fadeyi et al. (2009), filter removal efficiencies were estimated, not measured. In Coleman et al. (2008), SOA concentrations were estimated only with counts for diameters $\leq 0.4 \mu\text{m}$. Finally, Li et al. (2002) reported a range of

ventilation rates, and those in Table 3 are midrange values.

Results of Monte Carlo analyses

For the Monte Carlo analysis of each scenario, we ran 10 000 steady state and 10 000 transient cases. Table 4 lists summary statistics for results by scenario, including for C_{O_3} , C_{terp} , C_{Mb} , and C_{SOA} the 10th, 50th, and 90th percentiles, as well as the geometric mean and geometric standard deviation, for the resulting lognormal distributions. Transient results are peak values occurring during the modeled time. Ozone is of outdoor origin, so C_{O_3} for R1 is higher than R2/R3 because of the higher air exchange rate of R1; being of indoor origin, the reverse is true for C_{terp} . Transient C_{terp} values are much larger than steady-state values, reflecting the difference in the mass of terpenoid emitted in a pulse fashion by the use of the cleaning product vs. the steady emission of the air freshener. For transient cases, the impact of the air exchange rate is less and C_{terp} are similar for scenarios with different air exchange rates. For d-limonene vs. α -pinene, values of C_{O_3} and C_{terp} are slightly lower as the reaction rate

Table 4 Results of Monte Carlo analyses, including the 10th, 50th, and 90th percentiles for predicted steady-state and transient concentrations, as well as the geometric mean (GM) and geometric standard deviation (GSD) for their lognormal fits

Parameter	Scenario ^a	Terpenoid ^b	Steady-state results					Transient results				
			10th%	50th%	90th%	GM	GSD	10th%	50th%	90th%	GM	GSD
C_{O_3} ^c (ppb)	R1	lim1	4.6	11	28	11	2.0	4.6	12	28	11	2.0
		apin	4.6	12	28	11	2.0	4.6	12	28	11	2.0
	R2, R3	lim1	1.1	3.8	13	3.7	2.6	1.2	4.2	13	4.1	2.5
		apin	1.2	4.0	13	4.0	2.5	1.3	4.2	13	4.1	2.5
	O1	lim1	2.6	6.8	18	6.8	2.1	2.7	7.1	19	7.1	2.1
		apin	2.7	7.0	19	7.0	2.1	2.8	7.2	19	7.2	2.1
C_{terp} (ppb)	R1	lim1	1.6	3.7	9.0	3.7	1.9	316	543	925	542	1.5
		apin	1.7	3.9	10	4.0	1.9	317	545	928	545	1.5
	R2, R3	lim1	4.7	15	45	15	2.4	343	583	991	583	1.5
		apin	5.2	16	48	16	2.3	344	585	992	584	1.5
	O1	lim1	3.3	7.6	19	7.8	1.9	333	572	971	570	1.5
		apin	3.6	8.2	20	8.4	1.9	335	573	972	572	1.5
C_{Mb} ($\mu\text{g}/\text{m}^3$)	R1	lim1, apin	1.3	3.0	6.3	2.9	1.8	1.3	3.0	6.3	2.9	1.8
	R2	lim1, apin	0.47	1.3	3.0	1.2	2.1	0.47	1.3	3.0	1.2	2.1
	R3	lim1, apin	8.2	20	56	21	2.1	8.2	20	56	21	2.1
C_{SOA} ($\mu\text{g}/\text{m}^3$)	O1	lim1, apin	0.54	1.6	3.9	1.5	2.2	0.54	1.6	3.9	1.5	2.2
		lim1	0.040	0.14	0.54	0.15	2.7	2.0	5.8	19	6.0	2.4
	R1	apin	0.016	0.061	0.25	0.062	2.9	1.0	3.4	11	3.4	2.5
		lim1	0.083	0.37	1.7	0.37	3.2	1.1	4.0	15	3.9	2.8
	R2	apin	0.026	0.13	0.65	0.13	3.5	0.45	2.3	9.6	2.1	3.4
		lim1	0.24	1.2	5.2	1.1	3.3	2.9	9.3	31	9.3	2.5
	R3	apin	0.12	0.55	2.3	0.52	3.1	1.9	5.7	16	5.6	2.3
		lim1	0.050	0.22	0.87	0.21	3.1	1.3	4.3	15	4.3	2.7
	O1	apin	0.015	0.080	0.37	0.077	3.5	0.53	2.5	10	2.3	3.2

Transient results are the peak predicted values.

SOA, secondary organic aerosol.

^aScenario R1: residence with natural ventilation air exchange, and organic particles from outdoors; R2: residence with infiltration and recirculation air exchange, and organic particles from outdoors; R3: same as R2 but with organic particles also from indoor smoking; and O1: office with infiltration, mechanical ventilation, and recirculation air exchange, and organic particles from outdoors. Input distributions for Monte Carlo runs are in Table 2.

^bThese labels correspond to the yield curves for d-limonene (lim1) and α -pinene (apin) in Table 1 and Figure 1.

^c C_{O_3} values are initial conditions of ozone during the transient scenarios, which were also the maxima.

constant for d-limonene ozonolysis is larger than for α -pinene. Organic particles have both an outdoor and a major indoor source in R3, so its C_{Mb} is much higher than either R1 or R2. The O1 scenario has an air exchange rate between that of R2/R3 and R1, and as such, its C_{O_3} , C_{terp} , and C_{Mb} are between values of those scenarios.

Results of C_{SOA} show large variability; for d-limonene, the range was 0.0013–138 $\mu\text{g}/\text{m}^3$, and for α -pinene, it was 0.00028–53 $\mu\text{g}/\text{m}^3$. Formation for d-limonene exceeds that of α -pinene because of larger d-limonene yields and ozone reaction rates. Transient C_{SOA} results are roughly one to two orders of magnitude greater than steady-state results because of higher C_{terp} from the more intense pulse emission. At steady state, C_{SOA} for R2 > R1 because of lower air exchange rates (Weschler and Shields, 2000), and R3 > R2 because of indoor smoking as a source of C_{Mb} , which increases the yield. However, for transient C_{SOA} , the trend is not the same. Even though R1 has a higher air exchange rate than R2, which usually suppresses indoor reaction products, the peak formation is higher in R1 because the increase in C_{O_3} is relatively higher than the decrease in C_{terp} . Results for O1 are near R2 results because of similar air exchange rates and C_{Mb} values.

To illustrate the variation in yields across scenarios, we displayed in Figure 3 box plots of the steady-state and peak transient yield distributions, along with their lognormal fits. Median values for d-limonene and α -pinene are similar, but ranges of yields are much higher for d-limonene because of the greater magnitude of Y_{lim1} at higher M_{org} . Transient peak yields are generally greater than steady-state yields, reflecting the higher values of C_{terp} owing to the modeled pulse emission. Yields are a function of the scenarios and range from near zero for R2 and O1 to ~ 0.6 for R3.

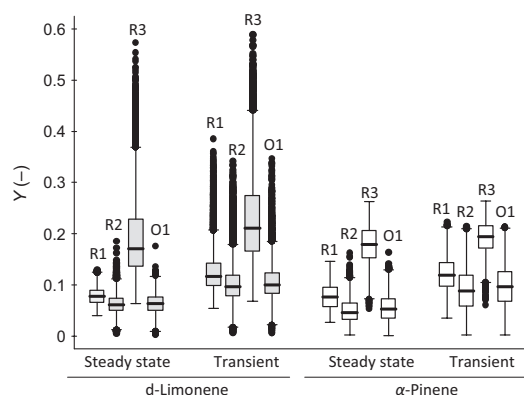


Fig. 3 Box plots and lognormal fits (GM, geometric mean; GSD, geometric standard deviation) for the d-limonene and α -pinene yield, Y (-), distributions for steady state and transient scenario Monte Carlo analyses. Abbreviations are for residential (R) and office (O) scenarios: R1 has indoor organic background particles (i.e., C_{Mb}) because of outdoor sources with natural ventilation; R2 has C_{Mb} from outdoor air infiltration; R3 has C_{Mb} from outdoor air infiltration and indoor smoking; and O1 has C_{Mb} from outdoor air infiltration and mechanical ventilation. Input parameters are listed in Table 2. Boxes describe 25th, 50th, and 75th percentiles, whiskers describe 5th and 95th percentiles, and dots are outliers

Consequently, assuming a constant yield to predict SOA formation is inappropriate and could either over- or under-predict formation, depending on the particular indoor environment being simulated. For instance, in high particle environments, d-limonene has the potential to have quite large yields, even when the reactant concentrations are relatively low.

We conducted a sensitivity analysis for the yield with a linear regression on parameters that influence SOA formation (i.e., terms in Equation 5 with Equation 6 substituted) by scenario. Standardized regression coefficients (SRC) were computed by normalizing the linear regression coefficients so that variances were equal to 1. These SRCs can have values from -1 to $+1$, and for them to be a valid measure of sensitivity, $R^2 \geq 0.7$ for linear fits (Saltelli et al., 2006), which was the case for all yields across all scenarios ($R^2 = 0.77$ – 0.96). For each input parameter, SRCs have these meanings on the yields: (i) $(\text{SRC})^2$ is the relative variance contribution; (ii) high $|\text{SRC}|$ indicates a large influence, while an $|\text{SRC}|$ near zero indicates no influence; and (iii) an input with a $-\text{SRC}$ changes the yield negatively and a $+\text{SRC}$ positively. Table 5 lists the SRCs for input parameters with $\text{SRC} \geq 0.1$ (i.e., ≥ 1 % effect on Y). For steady-state yields, C_{Mb} has the largest effect, while for peak yields, C_{O_3} at the time of terpenoid release has the largest effect, except when large indoor sources of background particles exist.

Model uncertainties and future work

The models perform well within our validation set but need refinement to increase their predictive ability. We neglected temperature variation indoors, and decreasing temperature will increase the yield (Leungsakul et al., 2005; Sarwar and Corsi, 2007). Variations in relative humidity (RH) were neglected; however, RH

Lognormal fits for yield distributions					
Scenario	Terpenoid	Steady state		Transient	
		GM	GSD	GM	GSD
R1	lim1	0.076	1.3	0.12	1.3
	pin	0.073	1.4	0.11	1.3
R2	lim1	0.059	1.4	0.096	1.5
	pin	0.043	1.8	0.079	1.8
R3	lim1	0.18	1.4	0.21	1.4
	pin	0.17	1.2	0.19	1.2
O1	lim1	0.059	1.5	0.10	1.4
	pin	0.047	1.8	0.086	1.7

Table 5 Standardized regression coefficients (SRC) of linear models of steady-state (SS) and peak transient (T) yields for inputs directly affecting SOA formation, listed by Monte Carlo scenarios

Parameter ^a	Terpenoid ^b	Scenario ^c R1		Scenario R2		Scenario R3		Scenario O1	
		SS	T	SS	T	SS	T	SS	T
C_{O_3}	lim1	0.077	0.87	0.24	0.90	0.049	0.44	0.15	0.86
	apin	0.035	0.70	0.14	0.73	0.045	0.35	0.070	0.68
C_{terp}	lim1	0.10	0.26	0.23	0.19	0.043	0.086	0.16	0.20
	apin	0.050	0.30	0.13	0.23	3.9E-04	0.091	0.081	0.24
C_{Mb}	lim1	0.96	0.35	0.75	0.27	0.91	0.84	0.78	0.32
	apin	0.97	0.56	0.91	0.43	0.70	0.67	0.89	0.46
λ_i	lim1	–	–	–0.14	–0.37	–0.095	–0.24	0.0042	–0.049
	apin	–	–	–0.072	–0.31	–0.23	–0.30	0.0063	–0.038
λ_n	lim1	–0.037	–0.28	–	–	–	–	–	–
	apin	–0.014	–0.27	–	–	–	–	–	–
λ_v	lim1	–	–	–	–	–	–	–0.024	–0.23
	apin	–	–	–	–	–	–	–0.0036	–0.19
$\eta_{SOA} \lambda_r$	lim1	–	–	–0.23	–0.24	–0.080	–0.15	–0.28	–0.25
	apin	–	–	–0.11	–0.24	–0.22	–0.28	–0.15	–0.29

Only influential parameters (ISRCI ≥ 0.1) are listed, with the most influential one for each scenario in bold.

SOA, secondary organic aerosol.

^aParameter β_{SOA} is excluded from this table as its ISRCI < 0.1 in all scenarios.

^bLabels correspond to the yield curves for d-limonene (Y_{lim1}) and α -pinene (Y_{apin}) in Table 1 and Figure 1.

^cScenario R1: residence with natural ventilation air exchange, and organic particles from outdoors; R2: residence with infiltration and recirculation air exchange, and organic particles from outdoors; R3: same as R2 but with organic particles also from indoor smoking; and O1: office with infiltration, mechanical ventilation, and recirculation air exchange, and organic particles from outdoors. Input distributions for Monte Carlo runs are in Table 2.

has little effect on SOA mass concentrations (Cocker et al., 2001; Leungsakul et al., 2005). Initial validation was only for the ozonolysis of a single reactive terpenoid, and future experiments will investigate the application of the models to mixed terpenoid environments, which would increase their potential uses if predictions are accurate. Future experiments should refine yields for indoor-relevant terpenoids at low M_{org} typical of indoors, as yields were derived at higher M_{org} . This work is especially necessary viewed in light of studies that have reported higher SOA formation than expected at low reactant concentrations for d-limonene (Waring et al., 2011) and α -pinene (e.g., Presto and Donahue, 2006). Finally, the ‘volatility basis set’ is a technique for predicting outdoor-formed SOA that has shown good ability at low M_{org} (e.g., Presto and Donahue, 2006), and future work will explore using this technique in indoor predictive models.

Conclusions

Two models, SOA-M1 and SOA-M2, were developed, which predict indoor SOA formation owing to single terpenoid ozonolysis with varying yields. Each model has its own strength. The first model is useful to predict transient SOA concentrations, and the second model is useful when solving for SOA concentrations at steady state. The models initially appear to effectively predict concentrations and were in agreement with published results. To estimate the possible ranges of yields and SOA concentrations in indoor settings, Monte Carlo analyses were performed for the ozonolysis of

d-limonene and α -pinene, considering steady-state and transient SOA formation in residential and office spaces. Results show that indoor use of terpenoid-rich products can lead to a large range of SOA concentrations and yields, and yields were a very strong function of background organic particles and indoor ozone concentration. The yield can be higher than what has been previously assumed, should not be considered as constant, and can be estimated with the methods in this article. It was also noted that most of the experimental research to determine yields has been carried out at high SOA concentrations unrealistic to most indoor settings and that there are large uncertainties in the application of fitted yield parameters at low concentrations.

Acknowledgements

We thank Charles J. Weschler for helpful discussions. This article is based upon work supported by the National Science Foundation (grant 1055584).

Supporting Information

Additional Supporting Information may be found in the online version of the article:

Data S1. Distributions for Monte Carlo analysis in Table 2.

Please note: Wiley-Blackwell are not responsible for the content or functionality of any supporting materials supplied by the authors. Any queries (other than missing material) should be directed to the corresponding author for the article.

References

- Alshawa, A., Russell, A.R. and Nizkorodov, S.A. (2007) Kinetic analysis of competition between aerosol particle removal and generation by ionization air purifiers, *Environ. Sci. Technol.*, **41**, 2498–2504.
- ASTM (1991) *Standard Guide for Evaluation of Indoor Air Quality Models*, Philadelphia, PA, American Society for Testing and Materials (D5157-91).
- Atkinson, R., Hasegawa, D. and Aschmann, S.M. (1990) Rate constants for the gas-phase reactions of O₃ with a series of monoterpenes and related compounds at 296 ± 2 K, *Int. J. Chem. Kinet. I*, **22**, 871–887.
- Chen, X. and Hopke, P.K. (2009) Secondary organic aerosol from α -pinene ozonolysis in dynamic chamber system, *Indoor Air*, **19**, 335–345.
- Chen, X. and Hopke, P.K. (2010) A chamber study of secondary organic aerosol formation by limonene ozonolysis, *Indoor Air*, **20**, 320–328.
- Chen, X., Hopke, P.K. and Carter, W.P.L. (2011) Secondary organic aerosol from ozonolysis of biogenic volatile organic compounds: chamber studies of particle and reactive oxygen species formation, *Environ. Sci. Technol.*, **45**, 276–282.
- Cocker, D.R., Clegg, S.L., Flagan, R.C. and Seinfeld, J.H. (2001) The effect of water on gas-particle partitioning of secondary organic aerosol. Part I: α -pinene/ozone system, *Atmos. Environ.*, **35**, 6049–6072.
- Coleman, B.K., Lunden, M.M., Destailhats, H. and Nazaroff, W.W. (2008) Secondary organic aerosol from ozone-initiated reactions with terpene-rich household products, *Atmos. Environ.*, **42**, 8234–8245.
- Destailhats, H., Lunden, M.M., Singer, B.C., Coleman, B.K., Hodgson, A.T., Weschler, C.J. and Nazaroff, W.W. (2006) Indoor secondary pollutants from household product emissions in the presence of ozone: a bench-scale chamber study, *Environ. Sci. Technol.*, **40**, 4421–4428.
- Fadeyi, M.O., Weschler, C.J. and Tham, K.W. (2009) The impact of recirculation, ventilation and filters on secondary organic aerosols generated by indoor chemistry, *Atmos. Environ.*, **43**, 3538–3547.
- Griffin, R.J., Cocker, D.R., Flagan, R.C. and Seinfeld, J.H. (1999) Organic aerosol formation from the oxidation of biogenic hydrocarbons, *J. Geophys. Res.*, **104**, 3555–3567.
- Hinds, W.C. (1999) *Aerosol Technology: Properties, Behavior, and Measurement of Airborne Particles*, New York, Wiley.
- Hoffmann, T., Odum, J.R., Bowman, F. and Collins, D. (1997) Formation of organic aerosols from the oxidation of biogenic hydrocarbons, *J. Atmos. Chem.*, **26**, 189–222.
- Holcomb, L.C. (1993) Indoor air quality and environmental tobacco smoke: concentration and exposure, *Environ. Int.*, **19**, 9–40.
- Kroll, J.H. and Seinfeld, J.H. (2005) Representation of secondary organic aerosol laboratory chamber data for the interpretation of mechanisms of particle growth, *Environ. Sci. Technol.*, **39**, 4159–4165.
- Lai, A.C.K. and Nazaroff, W.W. (2000) Modeling indoor particle deposition from turbulent flow onto smooth surfaces, *J. Aerosol Sci.*, **31**, 463–476.
- Lee, K., Vallarino, J., Dumyahn, T., Ozkaynak, H. and Spengler, J. (1999) Ozone decay rates in residences, *J. Air Waste Manage.*, **49**, 1238–1244.
- Lee, S.C., Lam, S. and Kin Fai, H. (2001) Characterization of VOCs, ozone, and PM₁₀ emissions from office equipment in an environmental chamber, *Build. Environ.*, **36**, 837–842.
- Leungsakul, S., Jaoui, M. and Kamens, R.M. (2005) Kinetic mechanism for predicting secondary organic aerosol formation from the reaction of d-limonene with ozone, *Environ. Sci. Technol.*, **39**, 9583–9594.
- Li, T.-H., Turpin, B.J., Shields, H.C. and Weschler, C.J. (2002) Indoor hydrogen peroxide derived from ozone/d-limonene reactions, *Environ. Sci. Technol.*, **36**, 3295–3302.
- Liu, D.-L. and Nazaroff, W.W. (2001) Modeling pollutant penetration across building envelopes, *Atmos. Environ.*, **35**, 4451–4462.
- Morrison, G.C., Shaughnessy, R. and Shu, S. (2011) Setting maximum emission rates from ozone emitting consumer appliances in the United States and Canada, *Atmos. Environ.*, **45**, 2009–2016.
- Murray, D.M. and Burmaster, D.E. (1995) Residential air exchange rates in the United States: empirical and estimated parametric distributions by season and climatic region, *Risk Anal.*, **15**, 459–465.
- Nazaroff, W.W. and Weschler, C.J. (2004) Cleaning products and air fresheners: exposure to primary and secondary air pollutants, *Atmos. Environ.*, **38**, 2841–2865.
- Ng, N.L., Kroll, J.H., Keywood, M.D., Bahreini, R., Varutbangkul, V., Flagan, R.C., Seinfeld, J.H., Lee, A. and Goldstein, A.H. (2006) Contribution of first- versus second-generation products to secondary organic aerosols formed in the oxidation of biogenic hydrocarbons, *Environ. Sci. Technol.*, **40**, 2283–2297.
- Odum, J.R., Hoffmann, T., Bowman, F., Collins, D., Flagan, R.C. and Seinfeld, J.H. (1996) Gas/particle partitioning and secondary organic aerosol yields, *Environ. Sci. Technol.*, **30**, 2580–2585.
- Persily, A.K., Gorfain, J. and Brunner, G. (2006) Survey of ventilation rates in office buildings, *Build. Res. Inf.*, **34**, 459–466.
- Polidori, A., Turpin, B.J., Lim, H., Cabada, J.C., Subramanian, R., Pandis, S.N. and Robinson, A.L. (2006) Local and regional secondary organic aerosol: insights from a year of semi-continuous carbon measurements at Pittsburgh, *Aerosol Sci. Technol.*, **40**, 861–872.
- Pope, C.A. and Dockery, D.W. (2006) Health effects of fine particulate air pollution: lines that connect, *J. Air Waste Manage.*, **56**, 709–742.
- Presto, A.A. and Donahue, N.M. (2006) Investigation of α -pinene + ozone secondary organic aerosol formation at low total aerosol mass, *Environ. Sci. Technol.*, **40**, 3536–3543.
- Riley, W.J., Mckone, T.E., Lai, A.C.K. and Nazaroff, W.W. (2002) Indoor particulate matter of outdoor origin: importance of size-dependent removal mechanisms, *Environ. Sci. Technol.*, **36**, 200–207.
- Saltelli, A., Ratto, M., Tarantola, S. and Campolongo, F. (2006) Sensitivity analysis practices: strategies for model-based inference, *Reliab. Eng. Syst. Saf.*, **91**, 1109–1125.
- Sarwar, G. and Corsi, R. (2007) The effects of ozone/limonene reactions on indoor secondary organic aerosols, *Atmos. Environ.*, **41**, 959–973.
- Sarwar, G., Corsi, R., Allen, D. and Weschler, C. (2003) The significance of secondary organic aerosol formation and growth in buildings: experimental and computational evidence, *Atmos. Environ.*, **37**, 1365–1381.
- Singer, B.C., Coleman, B.K., Destailhats, H., Hodgson, A.T., Lunden, M.M., Weschler, C.J. and Nazaroff, W.W. (2006a) Indoor secondary pollutants from cleaning product and air freshener use in the presence of ozone, *Atmos. Environ.*, **40**, 6696–6710.
- Singer, B.C., Destailhats, H., Hodgson, A.T. and Nazaroff, W.W. (2006b) Cleaning products and air fresheners: emissions and resulting concentrations of glycol ethers and terpenoids, *Indoor Air*, **16**, 179–191.
- Stephens, B., Siegel, J.A. and Novoselac, A. (2011) Operational characteristics of residential and light-commercial air-conditioning systems in a hot and humid climate zone, *Build. Environ.*, **46**, 1972–1983.
- Wainman, T., Zhang, J., Weschler, C.J. and Liou, P.J. (2000) Ozone and limonene in indoor air: a source of submicron particle exposure, *Environ. Health Perspect.*, **108**, 1139–1145.
- Waring, M. and Siegel, J. (2008) Particle loading rates for HVAC filters, heat

- exchangers, and ducts, *Indoor Air*, **18**, 209–224.
- Waring, M.S. and Siegel, J.A. (2010) The influence of HVAC systems on indoor secondary organic aerosol formation, *ASHRAE Trans.*, **116**, 556–571.
- Waring, M.S. and Siegel, J.A. (2011) The effect of an ion generator on indoor air quality in a residential room, *Indoor Air*, **21**, 267–276.
- Waring, M.S., Siegel, J.A. and Corsi, R.L. (2008) Ultrafine particle removal and generation by portable air cleaners, *Atmos. Environ.*, **42**, 5003–5014.
- Waring, M.S., Wells, J.R. and Siegel, J.A. (2011) Secondary organic aerosol formation from ozone reactions with single terpenoids and terpenoid mixtures, *Atmos. Environ.*, **45**, 4235–4242.
- Weschler, C.J. (2000) Ozone in indoor environments: concentration and chemistry, *Indoor Air*, **10**, 269–288.
- Weschler, C.J. and Nazaroff, W.W. (2008) Semivolatile organic compounds in indoor environments, *Atmos. Environ.*, **42**, 9018–9040.
- Weschler, C.J. and Shields, H.C. (1996) Production of hydroxyl radical in indoor air, *Environ. Sci. Technol.*, **30**, 3250–3258.
- Weschler, C.J. and Shields, H.C. (1999) Indoor ozone/terpene reactions as a source of indoor particles, *Atmos. Environ.*, **33**, 2301–2312.
- Weschler, C.J. and Shields, H.C. (2000) The influence of ventilation on reactions among indoor pollutants: modeling and experimental observations, *Indoor Air*, **10**, 92–100.
- Yu, J., Cocker, D.R. III, Griffin, R.J., Flagan, R.C. and Seinfeld, J.H. (1999) Gas-phase ozone oxidation of monoterpenes: gaseous and particulate products. *J. Atmos. Chem.*, **34**, 207–258.
- Zuraimi, M.S., Weschler, C.J., Tham, K.W. and Fadeyi, M.O. (2007) The impact of building recirculation rates on secondary organic aerosols generated by indoor chemistry, *Atmos. Environ.*, **41**, 5213–5223.